ACS OMEGA

Open Access

http://pubs.acs.org/journal/acsodf

Article

Bioactive Fiber Foam Films from Cellulose and Willow Bark Extract with Improved Water Tolerance

Tia Lohtander,* Tetyana Koso, Ngoc Huynh, Tuomo Hjelt, Marie Gestranius, Alistair W. T. King, Monika Österberg, and Suvi Arola

Cite This: *ACS Omega* 2024, 9, 8255−8265

Read Online

ACCESS | Metrics & More | Article Recommendations | Supporting Information

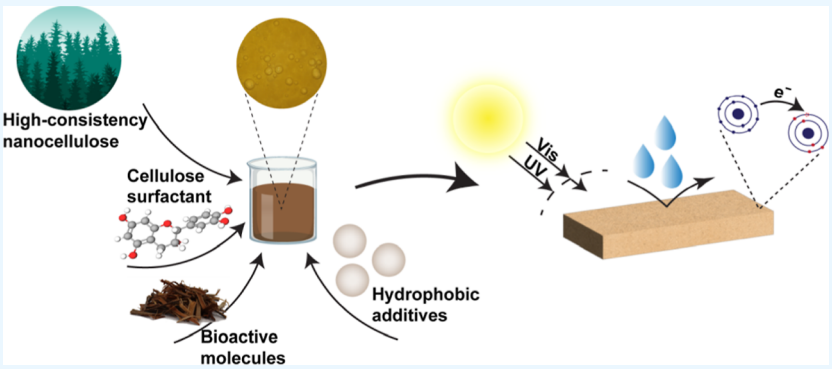

ABSTRACT: Cellulose-based materials are gaining increasing attention in the packaging industry as sustainable packaging material alternatives. Lignocellulosic polymers with high quantities of surface hydroxyls are inherently hydrophilic and hygroscopic, making them moisture-sensitive, which has been retarding the utilization of cellulosic materials in applications requiring high moisture resistance. Herein, we produced lightweight all-cellulose fiber foam films with improved water tolerance. The fiber foams were modified with willow bark extract (WBE) and alkyl ketene dimer (AKD). AKD improved the water stability, while the addition of WBE was found to improve the dry strength of the fiber foam films and bring additional functionalities, that is, antioxidant and ultraviolet protection properties, to the material. Additionally, WBE and AKD showed a synergistic effect in improving the hydrophobicity and water tolerance of the fiber foam films. Nuclear magnetic resonance (NMR) spectroscopy indicated that the interactions among WBE, cellulose, and AKD were physical, with no formation of covalent bonds. The findings of this study broaden the possibilities to utilize cellulose-based materials in high-value active packaging applications, for instance, for pharmaceutical and healthcare products or as water-resistant coatings for textiles, besides bulk packaging materials.

INTRODUCTION

There is constantly increasing interest in replacing fossil-based plastics with packaging materials from renewable sources. Cellulose is a widely utilized packaging material, and it is found, for instance, in the form of cardboard and cellophane. The advantages of cellulose in packages are its renewable origin, biodegradability, and recyclability.[1−3] The regulations and guidelines, such as UN sustainability goals, drive the packaging industry to transition toward more and more cellulose-based materials in the coming years.[4]

Low-density foam packaging materials are needed as protection for a variety of products, such as sensitive electronics, or as insulation material, for instance, for hot and cold food products. Apart from the advantage of low weight, the foam construct also provides insulation and a cushioning effect. Currently, petroleum-based low-density materials, such as expanded polystyrene and polyurethane, are widely utilized in foam-based materials. In addition to thick bulky foam packaging materials, foam films made from polyethylene and polyurethane have been utilized as protecting materials. In recent decades, foams made from cellulose-based materials, including pulp and cellulose nanofibers, have been investigated as sustainable alternatives.[5,6] In contrast to plastic foams, cellulose-based foams are sensitive to moisture and water due to the hygroscopic nature of cellulose fibers with hydroxyl group-rich surfaces.[7,8] The water sensitivity has been altered successfully with various surface modifications, such as noncovalent adsorption of hydrophobic compounds or covalent modification, including the esterification of cellulose

Received: November 9, 2023
Revised: January 24, 2024
Accepted: January 26, 2024
Published: February 9, 2024

Scheme 1. Schematic illustration of the foaming and fiber foam film preparation. The main constituents of the foam were high-consistency nanocellulose, carboxymethyl cellulose, and methylcellulose. The foam was modified with willow bark extract and hydrophobizing agent alkyl ketene dimer.

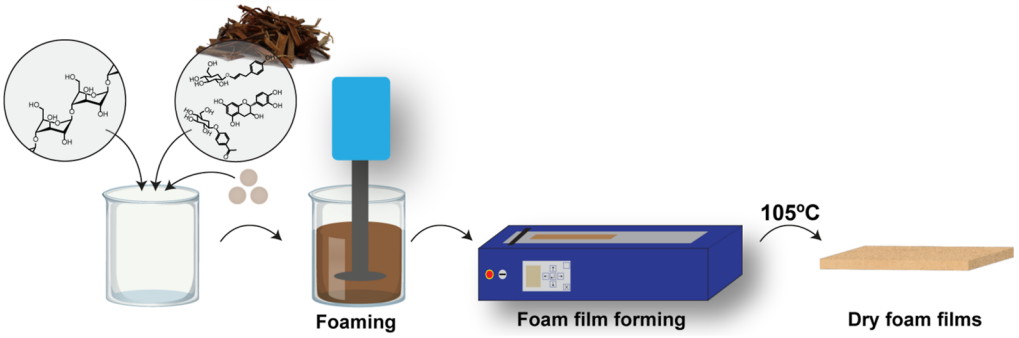

and grafting of hydrophobic compounds to cellulose.[9−11] In paper production, the hydrophobicity of paper is commonly increased with a low-cost, nontoxic, and biodegradable sizing agent called alkyl ketene dimer (AKD). Previous studies utilizing AKD as a hydrophobizing agent in biomaterials have reported that the products are biodegradable.[12,13] The AKD can change the surface chemistry of cellulose fibers permanently as it binds covalently to the cellulose hydroxyl groups via an esterification reaction.[14]

The foaming of cellulose-based structures is commonly achieved by utilizing surfactants that lower the surface energy and stabilize the foam by accumulating at the air/liquid interface.[15] The available surfactants vary from cationic and anionic to nonionic compounds, of which the latter two have a less toxic character. The cellulose fibers themselves also contribute to the stabilization of the wet foam structure; first, by increasing the viscosity of the foam and second as stabilizing additives, i.e., Pickering agents, physically preventing the drainage of liquid from the foam's continuous phase.[16,17] The wet cellulose foams can be dried either by freeze-drying or at elevated temperatures after foaming.[18−20] Drying at elevated temperatures is more feasible, as freeze-drying is slow, costly, and less scalable compared to heating.

Occasionally, other properties, such as antimicrobial, antioxidant, and moisture-scavenging properties, are highly useful, and it is desirable to introduce these added functionalities to be incorporated into the materials to create active packaging.[21] For instance, valuable nutritional supplements, and healthcare products without preservatives can benefit from active packaging, prolonging their shelf life. Willows (*Salix* sp.) are fast-growing crops that have been utilized, for instance, for medicinal purposes and energy production.[22,23] Instead of burning the valuable biomass, the willow could be fractionated into fiber and extractive feeds for more-resource wise utilization.[24]

In this work, we produced self-standing thin fiber foam films from high-consistency cellulose nanofibrils (CNF), carboxymethyl cellulose (CMC), and methylcellulose (MC). Willow bark extract (WBE) was added to the system to bring bioactive properties in the resulting fiber foam films. WBE is an aqueous solution of polyphenols and monosugars, which increase the viscosity of the CNF hydrogels.[25] Therefore, it was hypothesized that the WBE would influence the mechanical properties of the dry foam as well. Herein, we show that the WBE increased the mechanical strength of the fiber foams and provided protection against UV radiation and oxidation to the foams. Moreover, we show that the moisture sensitivity of the dry foam can be tuned with AKD and that the combination of AKD and willow bark can improve water resistance further. We present a novel approach that utilizes the synergistic effect of AKD and polyphenol-rich WBE for creating lightweight, self-standing, cellulose-based fiber foam films with improved hydrophobicity. The concept of functionalizing cellulose-based films by WBE has been presented earlier.[25,26] The novelty of this work lies in creating a self-standing foam structure from a high-consistency CNF with bioactive functionalities. The foam structure enables the use of less material compared to dense films, and the high solids content of the CNF grade utilized here allows the formation of stable wet foams. Additionally, due to the lower water content compared to native CNF grades, the drying of the structures requires less energy. The achieved properties, combined with a simple and scalable process, enable new opportunities to use cellulose-based foams in active packaging materials.

MATERIALS AND METHODS

Materials. High-consistency nanocellulose (CNF) was prepared from never-dried bleached softwood pulp with enzymatic fibrillation technology.[27] Native cellulose nanofibrils (nCNF) used for rheological tests were prepared from never-dried bleached hardwood pulp from a Finnish mill, following the procedure of Österberg et al.[28] The wood pulp, after being washed into sodium form, was refined using a Voith refiner (Heidenheim, Germany) and underwent six passes of mechanical fibrillation with an M-110P fluidizer (Microfluidics, Newton, MA). WBE was prepared from the bark of two-year-old willow hybrids (Klara, harvested in Kouvola, Finland), kindly provided by Carbons Finland Oy. Briefly, the bark was hot water extracted at 80 °C for 50 min according to the previously published method.[29] Then the extract was filtrated (filter paper, retention 12−15 μm) and centrifuged (4.500 g, 20 min, 21 °C) to remove residual solids, and the extract was freeze-dried to powder and stored at −20 °C. CMC, MC, ABTS (2,2′-azino-bis(3-ethylbenzothiazoline-6-sulfonic acid) diammonium salt), sodium persulfate, D-sorbitol, NMR solvents (specifically CH3OH-d_4 and DMSO-d_6), and tannic acid were obtained from Sigma-Aldrich. AKD (Aquapel 320) was obtained from Solenis LCC (USA). A homologically produced *Trametes hirsuta* laccase (*Th*L) with a catalytic activity of 5533 nkat ml^{-1} and a protein concentration of 3.5 g L^{-1} was purified with a method described elsewhere.[30] Tetra-*n*-butylphosphonium acetate ([P_{4444}][OAc]) was synthesized as

https://doi.org/10.1021/acsomega.3c08906
ACS Omega 2024, 9, 8255−8265

described in the literature,[31] from tetrabutylphosphonium bromide (99%, obtained from TCI Europe) and silver(I) acetate (99%, obtained from abcr). Deionized water was used in all experiments.

Fiber Foam Preparation and Characterization. The self-standing fiber foam film composites were produced according to Scheme 1. Ten g of high-consistency CNF with a dry solid content of 21.5%, 7 g of 1%(w/w) CMC aqueous solution, 1.6 g of 50%(w/w) sorbitol aqueous solution, and WBE and AKD were first dispersed thoroughly using a Dispermat (VMA-Getzmann GmbH, Germany), followed by the addition of 5 g of 1%(w/w) aqueous solution of MC, and then foamed for 2 min using a Dispermat (6500 rpm). The WBE was added to the system with a ratio of 1:2 or 1:4 (CNF/WBE, dry solids weight), and the amount of AKD was 2% of the CNF and CMC dry solid contents. The role of sorbitol in foams was to bring flexibility, while the CMC was hypothesized to stabilize foams further by hindering the drainage of water. Based on previous work, the laccase enzyme was also tested to improve WBE network formation.[25] The viscosity of foam systems, including CNF, CMC, sorbitol, MC, and WBE, before foaming was measured using a Brookfield Viscometer RVDV-III Ultra (Brookfield AMETEK Inc., USA) with a spindle size of 06 and a speed of 50 rpm. The viscosity reading was recorded at 10 s in duplicate. The complex viscosity of the 1.2%(w/w) nCNF hydrogel with varying concentrations of WBE was recorded with an Anton Paar MCR302 rheometer with a smooth 25 mm plate-to-plate geometry. The measurements were carried out in duplicate.

Foam Film Preparation and Characterization. The self-standing fiber foam films were prepared on polyethylene terephthalate (PET) films using a film applicator (Coatmaster 510, Erichsen, Germany) with a 2 mm comb and dried in an oven (Model UF110 Memmert GmbH, Germany) at 105 °C for 20 min. After drying, the fiber-foam films were peeled off the PET substrate, and their dry thickness was measured using an L&W micrometer (Lorentzen & Wettre, Sweden). The percentage shrinkage in thickness was calculated by comparing the achieved dry thickness to the wet thickness of 2 mm. The air content of wet foams was defined gravimetrically by filling a cup with a known volume of freshly prepared foam. The wet foams were imaged with an optical microscope (Nikon Eclipse Ci-POL, Nikon Instruments Inc., Japan) using 4× magnification.

Mechanical Properties of Fiber Foam Films. The density of dry fiber foam films was determined gravimetrically, and the porosity of foams was determined using the following equation

$$\text{Porosity}\ (\%) = \left(1 - \frac{\rho_f}{\rho_c}\right) \times 100 \tag{1}$$

in which ρ_f is the density of the dried foam, and ρ_c is the density of cellulose (1.5 g cm^{-3}). Although the foam films contained small amounts of other additives, the main material was cellulose (>50%), and thus, the density was compared to the value of pure cellulose. The mechanical properties were measured using a tensile tester (Lloyd LS5, Ametek, USA) with a 100 N load cell, 50 mm gauge length, and 5 mm min^{-1} elongation rate. The dry-fiber foam films were cut into 15 × 70 mm specimens using a surgical blade. The samples were stored at 23 °C and 50% relative humidity for at least 1 day before running the measurements. All values were determined from triplicate samples.

Characterizations of Fiber Foam Films. The microstructure of cross-sections of dry fiber foam films was imaged using field emission scanning electron microscopy (FE-SEM, Zeiss Merlin, Germany) at a 2 kV accelerating voltage in secondary electron mode with an in-lens detector. For the cross-sectional images, a small precut was cut on one side of the film, followed by freezing the film in liquid nitrogen, and finally, the film was pulled with pliers. The cut foams were fixed on carbon tape and sputtered with a 3 nm-thick Au/Pd coating.

The chemical structure of fiber foam films was analyzed in duplicate using attenuated total reflectance Fourier-transform infrared spectroscopy (ATR-FTIR, Nicolet iS50, Thermo Fisher Scientific, USA) equipped with a single-reflectance diamond ATR crystal.

Starting materials, such as CNF, WBE, and AKD, all single compounds, as well as their composites, were analyzed to determine if new covalent bonds were formed (CNF with AKD, WBE with AKD, or all three components prepared in ratios and conditions described earlier) by solution-state nuclear magnetic resonance (NMR) spectroscopy. Spectra were acquired using a Bruker AVANCE III 500 MHz spectrometer equipped with a 5 mm broadband-optimized BBO 500 MHz S2 probe head. Spectral data was recorded at 25 and 65 °C to reduce the viscosity of cellulosic solutions, improve resolution, and assess changes in chemical shifts caused by elevated temperatures. Samples were at first dissolved, as described in the protocol, in the combination of tetra-*n*-butylphosphonium acetate and deuterated dimethyl sulfoxide (electrolyte [P_{4444}][OAc]/DMSO-d_6 in mass ratio 1:4), due to the difficulties with cellulose dissolution in the conventional NMR solvents.[31] Also, pure DMSO-d_6 and MeOH-d_4 were used when possible for the samples.

For each of the samples, both the quantitative ^{1}H spectrum and the diffusion-edited ^{1}H spectrum were acquired. The standard "zg30" pulse program from the Bruker library was used for ^{1}H acquisitions, with relaxation delay D1 set to 10 s for prolonged peak quantitation. For the diffusion-edited ^{1}H spectrum, a 1D sequence was applied for diffusion measurement using stimulated echo and LED − "ledbpgp2s1d" pulse program from the Bruker library.[32] Bruker TopSpin 4.2.0 (https://bruker.com/) and MestReNova 14.3.1 (https://mestrelab.com/) software packages were used for spectra processing and formatting. Almost all chemical shifts in ^{1}H (proton) and ^{13}C (carbon) scales were calibrated to the DMSO-d_6 signal of δ = 2.50; 39.52 ppm when applicable. Also, for further characterization of compounds, additional experiments were performed selectively (see the full data in Table S1).

Bioactive Properties. The ultraviolet protection factor (UPF) was determined according to the European standard EN 13758-1.[33] The transmittance of fiber foam films was determined sing a spectrophotometer (UV2600, Shimadzu, Japan) with an integrating sphere. The UPF was calculated using the following equation

$$UPF = \frac{\sum_{\lambda=290}^{\lambda=400} E(\lambda)\varepsilon(\lambda)\Delta\lambda}{\sum_{\lambda=290}^{\lambda=400} E(\lambda)T(\lambda)\varepsilon(\lambda)\Delta\lambda} \tag{2}$$

https://doi.org/10.1021/acsomega.3c08906
ACS Omega 2024, 9, 8255−8265

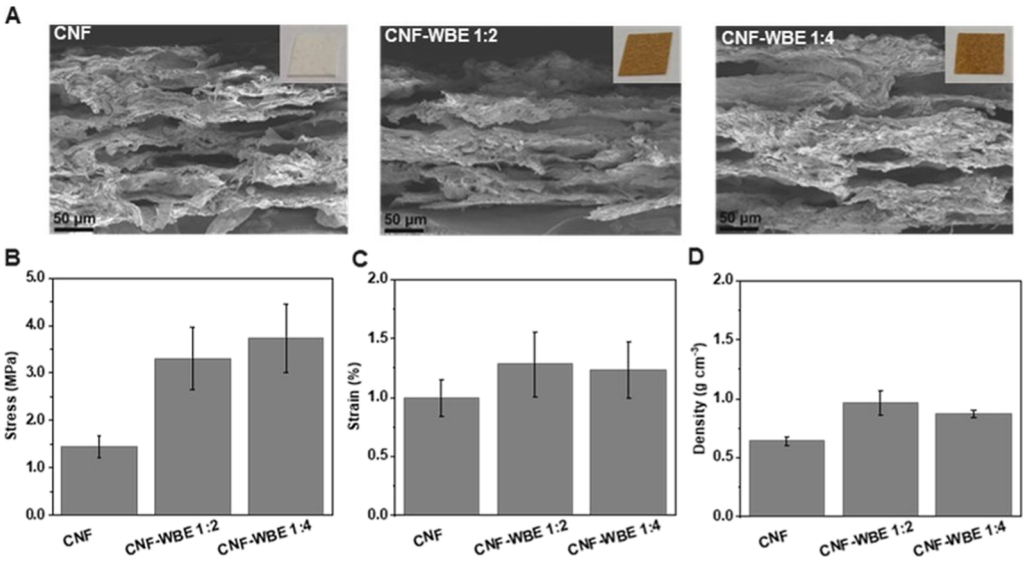

Figure 1. (A) Cross-sectional SEM micrographs of fiber foam films show the layered foam structure, with insets displaying photographs of corresponding dried films. (B) Tensile stress, (C) strain (%), and (D) density of fiber foam films from high-consistency cellulose nanofibers (CNF) and willow bark extract (WBE) with two different concentrations.

where $E(\lambda)$ is the solar irradiance, $\varepsilon(\lambda)$ is the erythema action spectrum, $T(\lambda)$ is the spectral transmittance at wavelength λ, and $\Delta\lambda$ is the wavelength interval.[32]

The antioxidant activity of dry fiber foam films and WBE was determined using the ABTS assay method described by Re et al. with small modifications.[35] First, the stock solution of the ABTS radical was prepared by mixing ABTS and sodium persulfate in water, which was allowed to react in the dark for 12−16 h. The ABTS radical stock was diluted until an absorbance of 0.7 au at 734 nm was reached. Circular fiber foam films with a diameter of 6 mm were mixed with 2 mL of diluted ABTS radical solution, and the absorbance was recorded after mixing samples in a rotator for 30 min. Pure WBE was mixed as a dry powder (2 mg) with the diluted ABTS radical solution. The radical scavenging activity of the samples was calculated using the following equation

$$\text{Radical scavening } (\%) = \frac{(1 - A_{sample})}{A_{ABTS}} \times 100 \quad (3)$$

where A_{sample} is the absorbance of the sample after reaction with ABTS radical solution, and A_{ABTS} is the absorbance of ABTS radical solution stock at 734 nm. Tannic acid (TA) was used as reference material, and the antioxidant activities of foams and WBE were reported as tannic acid equivalents based on the calibration curve from five TA concentrations between 0.1 and 2 μgmL^{-1}. All measurements were performed in triplicates.

Water Interactions. To assess the surface wetting properties, the water contact angles (WCA) of the fiber foam films were analyzed using an optical tensiometer (Attension Theta, Biolin Scientific, Finland) with the sessile drop method. The WCA was recorded from both sides of the fiber foam film with a drop volume of 5 μL. The WCA was determined from five parallel measurements. The water vapor sorption capacity of fiber foam films was studied using a gravimetric dynamic vapor sorption analyzer (DVS Resolution, Surface Measurements Systems Ltd., UK). To evaluate the effect of foam structure on water vapor sorption, a neat high-consistency CNF film and a film from high-consistency CNF, CMC, sorbitol, and MC were analyzed as control samples. The samples were stabilized in a desiccator for at least 2 days before the measurements. The measurements were carried out at 25 °C, and the relative humidity was increased from 0 to 90% and reduced back to 0% using a 15% step size. The sample weight was 10−13 mg, and each humidity step was continued until the mass change rate of 0.002%min^{-1} was reached. The equilibrium moisture sorption (%) was calculated as a percentage change in mass compared to the dry sample at 0% RH. The water resistance of films was experimented with by immersing the dry films in water for 24 h. The foams were photographed immediately after immersion, after 12 h, and after 24 h. The structural stability of the films was investigated by removing the fiber-foam film pieces from the water using tweezers.

RESULTS AND DISCUSSION

Fiber Foam Film Composites. Fiber foam films were produced via cast coating from a foam consisting of high-consistency CNF, CMC, MC, sorbitol, AKD, and varying amounts of WBE. CNF was expected to bring structural integrity to the foam, CMC to hinder gravity-driven drainage, sorbitol to plasticize the dry foam films, AKD to improve water tolerance, and WBE to both improve water tolerance and introduce protection against oxidation and UV degradation. The role of MC was to act as a foaming agent. Optimum foaming conditions and concentrations of CMC and MC had been established earlier, and for simplicity, these conditions were all kept constant to obtain comparable foams. The formed wet foams had spherical bubbles with an average diameter of 63−109 μm and air content ϕ below 64%, making them bubbly liquids by definition (Figure S1).[36] The AKD had an almost negligible effect on foam formation, but the addition of WBE reduced the air content down to half of the original air content ($\phi \sim 34-12\%$). The lower foamability was considered to be due to an increase in viscosity after the WBE addition. The viscosity was determined using two different methods, and they both indicated that incorporating WBE into the system increased the viscosity in the neat CNF system (Figure S2).

https://doi.org/10.1021/acsomega.3c08906
ACS Omega 2024, 9, 8255−8265

The increasing viscosity of the foam is commonly known to reduce the foaming capacity of the system.[37] A recent study proposed that the underlying mechanism behind increased viscosity is the reduced repulsion between cellulose fibrils due to the adsorption of WBE onto the fibril surfaces, which leads to the dehydration of hydrogel and consequently increased hydrogel strength.[38] As the viscosity increases in the system, it is more difficult to get the material to flow even with high shearing and to introduce air bubbles into the system. However, this increase in viscosity could also help stabilize the wet foam.

The wet foams were cast using a film applicator, and the resulting structures were hybrids of traditional films and foams. The dry fiber foam films had rough, porous surfaces, and the color of the films changed from white to light brown upon the addition of WBE (Figure 1A). The dried fiber foam films were conformable and could be bent, but folding caused creases like in paper (Video S1). On the microstructural level, the dry fiber foam films showed a sheeted layerlike structure with closed, elongated air pockets (Figure 1A). The mechanical properties of packaging materials are highly relevant, as the material needs to provide protection for the products that are packed in it, and thus, the fiber foam films were subjected to tensile tests. The tensile stress and strain values for the fiber foam films are presented in Figure 1B,C. In addition to increasing the hydrogel strength, the addition of WBE more than doubled the strength of dry fiber foam films. Likewise, the strain values were slightly higher when WBE was added to the composites. The addition of WBE increased the density of fiber foam films from 0.64 to 0.83−0.97, which is the main explanation for the increase in the mechanical strength (Table 1). As the fiber foam films' air content decreased, the number of discontinuities in the bulk matrix also decreased, resulting in an improvement in strength. As a comparison, the density of cellulose is ∼1.5 g cm^{-3}, and the densest CNF films can reach values close to cellulose.[39,40] The dry density of the fiber foam films correlated quite well with the air content of wet foams (Figure S3). The density of fiber foam film with a higher WBE concentration was slightly higher than that of fiber foam film with a lower WBE concentration (Figure 1D), and this is in line with the air contents of wet foams. As seen previously, AKD did not influence the foamability significantly, and thus, it did not have a notable effect on either mechanical properties (Figure S4) or density (Table 1). In hydrogels, laccase has been utilized to polymerize the phenolic compounds of WBE and improve the gel strength.[25] Laccase was also evaluated in this study, but it did not show any additional advantage for the foam as the film strength was not improved (Figure S4) and, therefore, it was not applied in further experiments.

Table 1. Density of dry fiber foam films and the shrinkage in thickness after drying.

	Thickness (μm)	Density (g cm^{-3})	Decrease in thickness (%)
CNF	238.7 ± 15.5	0.64 ± 0.04	88.07 ± 0.78
CNF AKD	248.3 ± 10.0	0.60 ± 0.02	87.58 ± 0.50
CNF-WBE 1:2	206.7 ± 5.7	0.97 ± 0.10	89.67 ± 0.28
CNF-WBE 1:2 AKD	217.0 ± 8.2	0.83 ± 0.02	89.15 ± 0.41
CNF-WBE 1:4	265.7 ± 2.1	0.87 ± 0.03	86.72 ± 0.10
CNF-WBE 1:4 AKD	263.7 ± 4.0	0.87 ± 0.06	86.82 ± 0.20

Bioactive Properties of Fiber Foam Films. Sunlight and free radicals can damage sensitive molecules; hence, they can shorten the shelf life of a variety of pharmaceutical and healthcare products. The polyphenolic compounds found in plant extracts can have antioxidant, antimicrobial, and sunlight-protecting properties since the role of these extracts as specialized metabolites is to protect the plant from external hazards.[41−43] The bark extractives of different wood species have been previously utilized in a variety of applications, including adhesives, absorbent materials, bio-oils, wood protective coatings, composite films, and textiles.[25,44−48] Herein, the polyphenolic-rich WBE was used to provide bioactive properties to the fiber foam films, which were studied in terms of protection from sunlight and antioxidant activity. The sunlight protection was evaluated by the UPF.[33] The UPF of samples can be classified as low (<15), good (15 ≤ UPF < 24), very good (24 ≤ UPF < 39), or excellent (≥40).[34] The fiber foam films with varying concentrations of WBE effectively blocked the radiation in the studied wavelength range (Figure 2A,B). The neat CNF foam showed a UPF value below 5, indicating that the sunlight protection without WBE is poor. The embedded WBE improved the fiber foam films' sunlight protection significantly, and the samples exhibited good UPF values. The mechanism behind good sunlight protection is the ability of WBE to efficiently absorb UV light, which is typical for phenolic compounds.[49] However, it is noteworthy that doubling the WBE concentration did not significantly improve the UPF values, and maximum sunlight protection was already achieved with the smaller amount of WBE.

In addition to the sunlight protection, the fiber foam films with WBE showed radical scavenging up to 80%, while WBE alone was able to scavenge almost all ABTS radicals, as the radical scavenging was ∼96% (Figure 2C). WBE alone was free in the solution and, therefore, more accessible to interact with ABTS radicals compared to WBE embedded in the CNF foam matrix. CNF foam without WBE was also able to scavenge some of the radicals, probably due to the physical entrapment of the dye in the foam rather than the actual radical reaction, but the addition of WBE improved the scavenging ability from 20 to 80%. Tannic acid was used as a reference compound in the antioxidant activity determination (Figure S5), and as the mass of samples was taken into account in the antioxidant activity calculations, the difference in antioxidant activity between free WBE and WBE embedded in the CNF matrix was more notable (Figure 2D). The WBE concentration was doubled to achieve the higher antioxidant activity; however, the results presented in Figure 3C,D showed that the increasing WBE content in the fiber foam film had only a minor influence on the radical scavenging. The minor difference is plausibly due to the more limited accessibility of WBE embedded in the foam, and thus, the excess antioxidant inside the fiber foam film matrix cannot participate actively in scavenging the ABTS radicals.

Chemical Composition of Functionalized Fiber Foams. The FTIR spectra of fiber foam films were measured to determine the presence of WBE and AKD and to define the changes in the chemical structure of fiber foam films upon their addition (Figure 3). The spectrum of neat CNF foam (Figure 3A) showed the typical absorptions of cellulose backbone (υ_{OH} 3340 cm^{-1}, υ_{CH} 2901, 1429 cm^{-1}, υ_{H2O}1641 cm^{-1}, υ_{C-O} 1160, 1054 cm^{-1}, $\upsilon_{\beta\text{-linkage}}$ 896 cm^{-1}).[50] The addition of WBE to the foam introduced new absorptions at 1605 and 1515 cm^{-1} (Figure 3A), which are attributed to the aromatic rings of

https://doi.org/10.1021/acsomega.3c08906
ACS Omega 2024, 9, 8255−8265

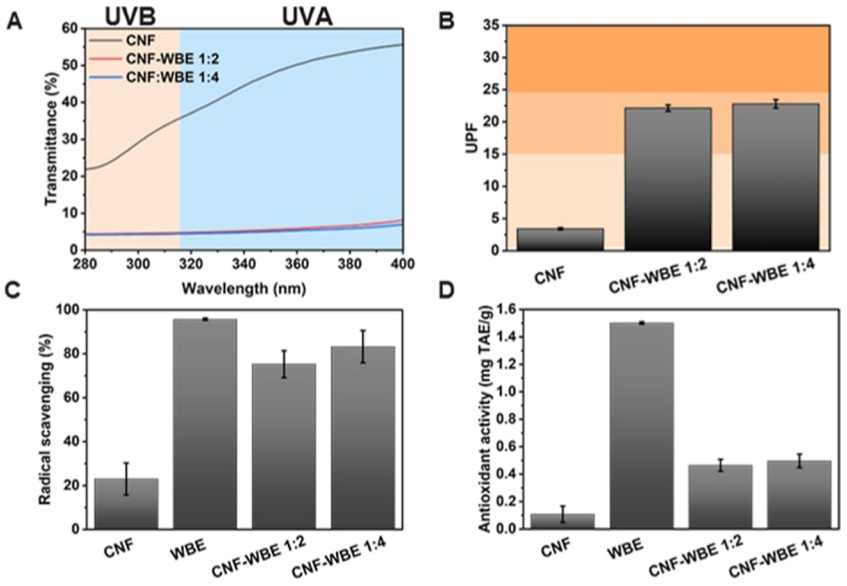

Figure 2. Bioactive properties of the fiber foam films made from high-consistency cellulose nanofibers (CNF) and willow bark extract (WBE). (A) Transmittance (%) of fiber foam films over the wavelength range 280−400 nm and (B) UPF of fiber foam films. (C) ATBS radical scavenging (%) ability and (D) antioxidant activity of fiber foam films as tannic acid equivalents.

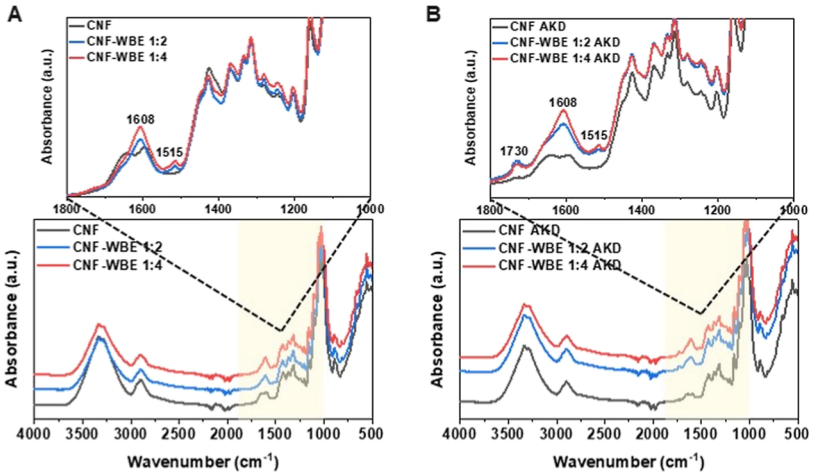

Figure 3. ATR-FTIR spectra of fiber foam films. (A) Foam of high-consistency cellulose nanofibers (CNF) with willow bark extract (WBE) with two different concentrations; and (B) same samples with the hydrophobizing agent AKD.

WBE. The interaction between polyphenolic WBE and CNF is based on the physical bonding (hydrogen, hydrophobic interaction, $\pi-\pi$ interaction, and electrostatic interactions[51,52]), and no sign of new covalent chemical bonds was observed in the spectra. However, AKD can interact through both physical and chemical interactions, according to the literature. The chemical interactions can be seen as the formation of β-ketone ester bonds at 1703 cm^{-1}, and the physical interactions of AKD can be seen at approximately 1600 and 1722 cm^{-1}, which are assigned to symmetric stretching of C═C and C═C stretching vibrations of AKD, respectively.[14,53,54] The absorption band at 1600 cm^{-1} due to the physical adhesion of AKD is difficult to distinguish from the spectra as a result of overlapping bands of CNF and WBE (Figure 3A,B). However, upon the addition of AKD (Figure 3B), especially in combination with WBE, a new shoulder appeared around 1720−1730 cm^{-1}, which indicates the presence of AKD in the foams. The intensity of the absorption band is rather low, which is due to the low dosage of AKD (2% of the CNF dry content). A similar absorption band was also observed in the spectra of pure WBE and CNF with AKD without the other compounds of the foam (Figure S6), indicating that the absorption band is due to AKD.

The applied dosage of AKD was low; and therefore, the amount of potential chemically bound AKD on CNF and WBE would most probably be below the detection limits of the FTIR technique. Consequently, the foams were further studied with NMR. As all the analyzed materials had to be dissolved, preferably in the same solvent as cellulose-containing materials, an electrolyte $[P_{4444}][OAc]$: DMSO-d_6 was used.[31] WBE dissolution in the electrolyte with subsequent heating resulted in a solution color change from brown to black, and spectral data demonstrated signs of material polymerization as broadened signals in the 6.0−7.5 ppm region of the proton spectrum (Figures S7 and S8). This was expected, as the electrolyte is a strong base, which, in combination with heating, can activate the condensation of polyphenolic compounds. Despite this, at least picein and triandrin were clearly identified

https://doi.org/10.1021/acsomega.3c08906
ACS Omega 2024, 9, 8255−8265

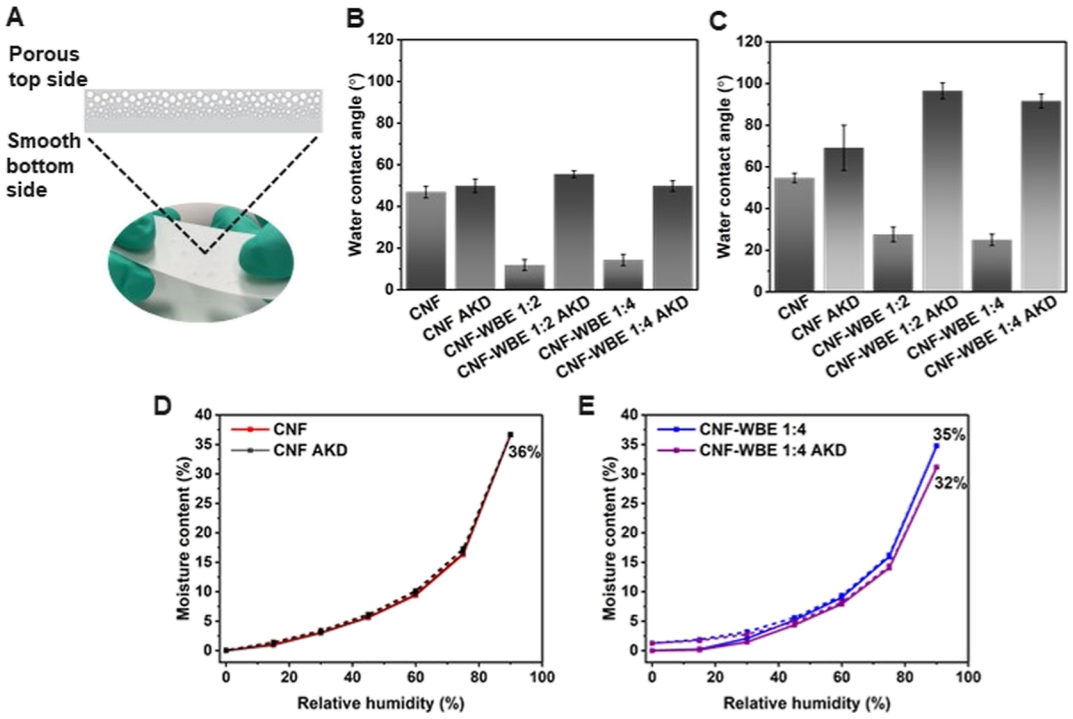

Figure 4. (A) Photograph of fiber foam film and a schematic illustration of their cross-sectional structure. (B) WCAs were measured at 10 s from the top side and (C) from the bottom side of the fiber foam films. (D) Moisture content of CNF and CNF−AKD fiber foam films, and (E) moisture content of fiber foam films with WBE and AKD measured using DVS. The adsorption curve is marked with a solid line, and the desorption curve is marked with a dashed line.

as the main components based on known literature.[29] The sample was also characterized at lower temperatures to ensure comparable assignments in relation to the literature. The sample was additionally dissolved in pure DMSO-d_6, and spectra were recorded. However, this confirmed only previous assignments, even with no colorization of the sample. Saccharide resonances were not resolved as well as in the electrolyte, which was also indicated by the poorer solubility of WBE in the pure solvent.

Spectral data of dissolved cellulose nanofibers (CNF) did not show any deviations from expected components with the presence of cellulose and hemicellulose resonances (xylose and mannose, Figures S9 and S10).[55,56] To identify possible chemical reactions among WBE, AKD, and CNF, their samples were prepared with the ratios and conditions described in Section 2.2. The product of the WBE and AKD combination was dissolved in DMSO-d_6 to avoid possible interference of the electrolyte with WBE. We could easily identify saturated long-chain peaks of AKD among proton resonances. Also, phenolic signals of picein were present, as well as triandrin; however, unsaturated signals CH-7, CH-8, and split CH_2-9 of triandrin were missing (Figure S11). Instead, the phenolic signals of triandrin were broadened. This can be explained by the reaction of (cross)polymerization at those moieties. Again, the characteristic broadening of peaks in the aromatic region was an indication that partial polymerization had occurred.

Acquired diffusion-edited ^{1}H NMR spectrum of the AKD and CNF reaction products was obtained. This experiment is routinely used to potentially identify covalent attachments between polymers and low-molecular-weight reactants. It indicated the presence of broadened signals of saturated AKDs' alkyl chains and was initially in agreement with previous literature data.[57] However, an insoluble waxlike material was persistent in the NMR tube and indicated the possible presence of micelles, which might also contribute to the signal in diffusion-edited ^{1}H NMR. To ensure that these resonances would not be micelle artifacts, a fresh sample was prepared with DCM prewash to ensure that unbound AKD would be removed. Spectral data for this new sample demonstrated a significant decrease in alkyl chain signals-obtained resonances indicated that the majority of the AKD was physisorbed to CNF (Figure S12). Any signs of the expected covalent bond characteristic CH signal (between two carbonyl groups) were absent or below the detection limit (for 2D data sets). Additionally, the CNF resonances overlapped with the sugar resonances of WBE, complicating the picture even more (Figures S13 and S14). Therefore, the formation of new covalent bonds could not be verified (Figure S13), and the interaction between CNF/WBE and AKD was assumed to be mainly physical or weak bonds.

Water Interactions. Water resistance and interactions are critical features of packaging materials. The major limiting factor hindering the replacement of plastic-based packaging materials with cellulose-derived materials is the hygroscopic character of cellulose and its low water tolerance. Therefore, both the surface-wetting properties and bulk sorption behavior of fiber foam films were determined using WCA and DVS measurements, respectively (Figure 4). It should be noted that the fiber foam films produced herein had two sides with rather different surface structures due to foam aging occurring during the foam drying. As the foam ages, the liquid begins to drain from the foam phase, and bubbles begin to grow, leading to the coarsening of the foam. Therefore, the bottom side of the dried fiber foam films, where the gravitation forces the liquid, became a smooth, film-like structure, while the top side of the fiber foam film has a coarse and porous surface structure

https://doi.org/10.1021/acsomega.3c08906
ACS Omega 2024, 9, 8255−8265

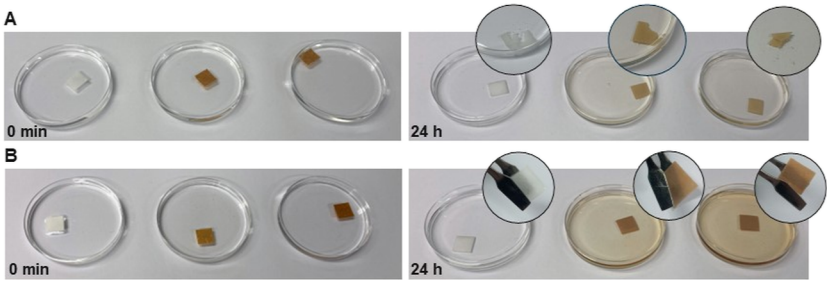

Figure 5. Qualitative water resistance test of fiber foam films at the time of immersion (0 min, left side pictures) and after 24 h of immersion (right side pictures) from (A, top panel) high consistency cellulose nanofibers (CNF, sample to the left on each image) and CNF with two different willow bark extract concentrations (CNF + WBE 1:2 middle sample, CNF + WBE 1:4 sample to the right on each image) and (B, bottom panel) the same fiber foam films also containing hydrophobizing agent AKD.

(Figure 4A). Due to this reason, the WCA and the wetting properties were notably different for the top and bottom sides of the samples (Figure 4B,C).

The WCA of neat CNF fiber foam films without any additives indicated that the foam is hydrophilic on both sides, although the WCA was slightly higher on the bottom side due to the smoother surface. As expected, upon the addition of hydrophobizing agent AKD, the contact angles increased on both sides, even though the influence was greater on the smoother bottom side than on the porous top side. On the top side, the porosity of the material had a more dominant influence on the wetting behavior than the surface chemistry of the AKD-modified CNF fibers. The WCA measurements revealed that the addition of hydrophilic WBE increased the hydrophilicity of the fiber foam films compared with the CNF fiber foam film. The WBE produced in the hot water extraction process is a highly hydrophilic compound, and therefore, the addition of hydrophilic WBE into the hydrophilic CNF matrix increased the corresponding weight portions of the hydroxyl groups on the surface that can interact with water molecules. The combination of both WBE and AKD surprisingly reduced the hydrophilicity of fiber foam films even more than AKD alone and made the smooth bottom side of the fiber foam film almost hydrophobic. The drying at elevated temperatures made WBE less water-soluble and hydrophobic (Figure S15), which alone did not increase the WCA of CNF-WBE films. On the bottom side, simultaneous use of AKD and WBE showed a synergistic effect, and the WCA increased notably. As the foams were cast on smooth PET film and the foam evolved during drying, we can expect that all the foams had similar smooth film-like surfaces on the bottom side. Therefore, the synergistic effect of AKD and WBE on the bottom side could be explained through the reactions occurring between hydroxyl groups rather than through the differences in the surface topography. Based on NMR results, both WBE and AKD interact with CNF only via physical forces. The physisorption occurs mainly via hydrogen bonding,[25] and this creates competing adsorption for water molecules as there are a limited number of OH sites available. The increased WCA suggests that this competing interaction changes the alignment of the WBE and causes the more hydrophobic domains of the WBE to face toward the air interface. This view is supported by another research, which argues that the hydrophobic domains of a polyphenolic compound, tannin from *Acacia mearnsii* bark, are oriented toward the surface while the hydrophilic domains adsorb on cellulose.[58] The bark of various Nordic tree species, in general, is rich in amphiphilic compounds.[59] Similar to any polyphenolic compound, the WBE consists of hydrophilic parts (OH groups) and more hydrophobic parts (aromatic rings). However, more research is needed to verify the exact mechanism behind the observed synergistic effects of WBE and AKD.

In addition to the surface wetting behavior, the bulk moisture sorption of fiber foam films was investigated using the DVS technique. A similar moisture sorption isotherm shape was observed for all fiber foam films despite the addition of WBE or AKD (Figure 4D,E). The moisture sorption capacity was higher in CNF fiber foam films and in CNF fiber foam film with only WBE, while upon the addition of both WBE and AKD, the sorption capacity of the fiber foam films was reduced. The isotherm shape of fiber foam films was more type III (Flory−Huggins) than the sigmoidal shape typical for lignocellulosic materials, including CNF, and additionally, the hysteresis, i.e., the difference between absorption and desorption curves, was minimal.[60] This indicates that the water interactions of the materials analyzed herein differ from the typical lignocellulosic behavior. The hysteresis commonly observed for lignocellulosic materials is explained to be due to sorption taking place in different material states, as the adsorption of water molecules onto the dry and collapsed matrix is lower than the desorption from the wet and swollen matrix, in which the water molecules strongly interact via hydrogen bonds.[61] The lack of hysteresis in this study can thus be assumed to be due to reduced dimensional changes during adsorption and desorption cycles. The once-dried foam with a porous structure retains a more open matrix structure and high accessibility for water adsorption. A compact film made of the same compounds and dried in the same conditions showed lower moisture uptake and distinguishable hysteresis, verifying that the lack of hysteresis in fiber foam films originated from the porous structure (Figure S16). The influence of structural swelling on sorption hysteresis has been addressed earlier elsewhere.[62] The fiber foam films were plasticized using sorbitol, which improves ductility not only by disturbing the intra- and intermolecular hydrogen bonding network but also by increasing the ability to absorb moisture.[63] The increase in moisture absorption ability given by the plasticizer can also contribute to the total moisture uptake of the fiber foam films.[64,65]

In addition to the surface wetting properties and bulk moisture sorption behavior, the water tolerance of the fiber foam films was qualitatively evaluated by immersing pieces of fiber foam films in water for 24 h. Without the hydrophobizing agent AKD, the immersed fiber foam films were very delicate; hence, the collection of intact films from the water bath after the test period was impossible (Figure 5A). The addition of

https://doi.org/10.1021/acsomega.3c08906
ACS Omega 2024, 9, 8255−8265

AKD improved the water tolerance of the films, and intact films could be collected and handled with a tweezer without disintegration after the test period (Figure 5B). WBE leached out of the films with and without AKD; however, in AKD-treated films, it seemed to be more pronounced. This supports the hypothesis about competing the physisorption of AKD and WBE onto CNF, as the more pronounced leaching indicates that WBE is more loosely bound when AKD is present in the foams. Due to the leaching, the system is not yet suitable for active packaging used for food or wet conditions, but it could be useful for applications where resistance to humid air is important.

CONCLUSIONS

This work presents a route to prepare lightweight, porous composite nanocellulose fiber foam films with improved water stability and functional properties, going beyond standard packaging materials. Each element of the film serves a purpose: high consistency CNF brings structural integrity, AKD improves water stability, and WBE functionalizes the fiber foam films. The fiber foam films were thoroughly characterized regarding their mechanical strength, and SEM images revealed a porous microstructure. The addition of AKD significantly improved the water stability of the films, as demonstrated by WCA, DVS, and immersion experiments. The addition of WBE brought functionality through sunlight protection and antioxidative properties. Interestingly, a synergetic effect between AKD and WBE was observed with regard to the surface hydrophobicity of the films. We hypothesize that due to the competing hydrogen bonding between CNF, AKD, and WBE, the hydrophobic domains of WBE oligomers face toward the air interface, which enhances the surface hydrophobicity. The presented fiber foam film approach enables hydrophobization and functionalization integrated into the foaming process, predicting feasible scalability and possibilities to expand the concept by introducing other functional components. We envision that these fiber foam materials could find use in novel applications where traditional fiber materials cannot be used due to their high moisture sensitivity. These applications could include, for example, active textile coatings besides conventional packaging and insulating coatings.

ASSOCIATED CONTENT

Supporting Information

The Supporting Information is available free of charge at https://pubs.acs.org/doi/10.1021/acsomega.3c08906.

Air contents and viscosities of wet foams, mechanical properties and ATR-FTIR spectra of additional fiber foam film samples, calibration curve used in antioxidant calculations, additional experimental details of the NMR study, ^{1}H and $^{1}H-^{13}C$ HSQC spectra of CNF, WBE, and AKD, photographs of CNF-WBE films dried in different conditions, moisture contents of films, and video of dry fiber foam film (PDF)

AUTHOR INFORMATION

Corresponding Author

Tia Lohtander − *Biomass Processing and Products, VTT Technical Research Centre of Finland Ltd, Espoo FI-02044, Finland;* orcid.org/0000-0003-2707-7692; Email: tia.lohtander-piispa@vtt.fi

Authors

Tetyana Koso − *Biomass Processing and Products, VTT Technical Research Centre of Finland Ltd, Espoo FI-02044, Finland*

Ngoc Huynh − *Department of Bioproducts and Biosystems, School of Chemical Engineering, Aalto University, Espoo FI-02044, Finland;* orcid.org/0000-0002-3814-6801

Tuomo Hjelt − *Biomass Processing and Products, VTT Technical Research Centre of Finland Ltd, Espoo FI-02044, Finland*

Marie Gestranius − *Biomass Processing and Products, VTT Technical Research Centre of Finland Ltd, Espoo FI-02044, Finland;* orcid.org/0000-0002-4348-8996

Alistair W. T. King − *Biomass Processing and Products, VTT Technical Research Centre of Finland Ltd, Espoo FI-02044, Finland*

Monika Österberg − *Department of Bioproducts and Biosystems, School of Chemical Engineering, Aalto University, Espoo FI-02044, Finland;* orcid.org/0000-0002-3558-9172

Suvi Arola − *Biomass Processing and Products, VTT Technical Research Centre of Finland Ltd, Espoo FI-02044, Finland;* orcid.org/0000-0003-4087-3837

Complete contact information is available at: https://pubs.acs.org/10.1021/acsomega.3c08906

Author Contributions

The manuscript was written through the contributions of all authors. All authors have given their approval to the final version of the manuscript.

Funding

This work was a part of the Academy of Finland's Flagship Programme under projects No. 318890 and 318891 (Competence Center for Materials Bioeconomy, FinnCERES).

Notes

The authors declare no competing financial interest.

ACKNOWLEDGMENTS

The authors would like to acknowledge Panu Lahtinen for providing the high-consistency nanocellulose and Martina Blomster-Andberg for providing the laccase enzyme.

REFERENCES

(1) Klemm, D.; Heublein, B.; Fink, H. P.; Bohn, A. Cellulose: Fascinating biopolymer and sustainable raw material. *Angew. Chem., Int. Ed.* **2005**, *44*, 3358−3393.

(2) Dufresne, A. Nanocellulose: A new ageless bionanomaterial. *Mater. Today* **2013**, *16* (6), 220−227.

(3) Kontturi, E.; Laaksonen, P.; Linder, M. B.; Nonappa; Gröschel, A. H.; Rojas, O. J.; Ikkala, O. Advanced Materials through Assembly of Nanocelluloses. *Adv. Mater.* **2018**, *30*, 1703779.

(4) United Nations. Transforming Our World: The 2030 Agenda for Sustainable Development A/RES/70/1, 2015. Available at: https://www.un.org/ga/search/view_doc.asp?symbol=A/RES/70/1&Lang=E.

(5) Pääkkö, M.; Vapaavuori, J.; Silvennoinen, R.; Kosonen, H.; Ankerfors, M.; Lindström, T.; Berglund, L. A.; Ikkala, O. Long and entangled native cellulose I nanofibers allow flexible aerogels and hierarchically porous templates for functionalities. *Soft Matter* **2008**, *4*, 2492−2499.

(6) Zheng, C.; Li, D.; Ek, M. Cellulose-fiber-based insulation materials with improved reaction-to-fire properties. *Nord. Pulp Pap. Res. J.* **2017**, *32*, 466−472.

(7) Klemm, D.; Kramer, F.; Moritz, S.; Lindström, T.; Ankerfors, M.; Gray, D.; Dorris, A. Nanocelluloses: A New Family of Nature-Based Materials. *Angew. Chem., Int. Ed.* **2011**, *50*, 5438−5466.
(8) Solhi, L.; Guccini, V.; Heise, K.; Solala, I.; Niinivaara, E.; Xu, W.; Mihhels, K.; Kröger, M.; Meng, Z.; Wohlert, J.; et al. Understanding Nanocellulose-Water Interactions: Turning a Detriment into an Asset. *Chem. Rev.* **2023**, *123* (5), 1925−2015.
(9) Shang, W.; Huang, J.; Luo, H.; Chang, P. R.; Feng, J.; Xie, G. Hydrophobic modification of cellulose nanocrystal via covalently grafting of castor oil. *Cellulose* **2013**, *20*, 179−190.
(10) Sehaqui, H.; Zimmermann, T.; Tingaut, P. Hydrophobic cellulose nanopaper through a mild esterification procedure. *Cellulose* **2014**, *21*, 367−382.
(11) Kontturi, K. S.; Biegaj, K.; Mautner, A.; Woodward, R. T.; Wilson, B. P.; Johansson, L. S.; Lee, K. Y.; Heng, J. Y. Y.; Bismarck, A.; Kontturi, E. Noncovalent surface modification of cellulose nanopapers by adsorption of polymers from aprotic solvents. *Langmuir* **2017**, *33*, 5707−5712.
(12) Van Nguyen, S.; Lee, B.-K. Polyvinyl alcohol/cellulose nanocrystals/alkyl ketene dimer nanocomposite as a novel biodegradable food packing material. *Macromolecules* **2022**, *207*, 31−39.
(13) Jaiswal, A. K.; Kumar, V.; Jansson, E.; Huttunen, O.-H.; Yamamoto, A.; Vikman, M.; Khakalo, A.; Hiltunen, J.; Behfar, M. H. Biodegradable Cellulose Nanocomposite Substrate for Recyclable Flexible Printed Electronics. *Adv. Electron. Mater.* **2023**, *9* (4), 2201094.
(14) Lindström, T.; Larsson, P. T. Alkyl ketene dimer (AKD) sizing - A review. *Nordic Pulp Pap. Res. J.* **2008**, *23*, 202−209.
(15) Wang, J.; Nguyen, A. v.; Farrokhpay, S. A critical review of the growth, drainage and collapse of foams. *Adv. Colloid Interface Sci.* **2016**, *228*, 55−70.
(16) Murray, B. S.; Ettelaie, R. Foam stability: Proteins and nanoparticles. *Curr. Opin. Colloid Interface Sci.* **2004**, *9*, 314−320.
(17) Lam, S.; Velikov, K. P.; Velev, O. D. Pickering stabilization of foams and emulsions with particles of biological origin. *Curr. Opin. Colloid Interface Sci.* **2014**, *19*, 490−500.
(18) Sehaqui, H.; Salajková, M.; Zhou, Q.; Berglund, L. A. Mechanical performance tailoring of tough ultra-high porosity foams prepared from cellulose I nanofiber suspensions. *Soft Matter* **2010**, *6*, 1824−1832.
(19) Cervin, N. T.; Andersson, L.; Ng, J. B. S.; Olin, P.; Bergström, L.; Wågberg, L. Lightweight and strong cellulose materials made from aqueous foams stabilized by nanofibrillated cellulose. *Biomacromolecules* **2013**, *14*, 503−511.
(20) Martoïa, F.; Cochereau, T.; Dumont, P. J. J.; Orgéas, L.; Terrien, M.; Belgacem, M. N. Cellulose nanofibril foams: Links between ice-templating conditions, microstructures and mechanical properties. *Mater. Des.* **2016**, *104*, 376−391.
(21) Yildirim, S.; Röcker, B.; Pettersen, M. K.; Nilsen-Nygaard, J.; Ayhan, Z.; Rutkaite, R.; Radusin, T.; Suminska, P.; Marcos, B.; Coma, V. Active Packaging Applications for Food. *Compr. Rev. Food Sci. Food Saf.* **2018**, *17*, 165−199.
(22) Mahdi, J. G. Medicinal potential of willow: A chemical perspective of aspirin discovery. *J. Saudi Chem. Soc.* **2010**, *14*, 317−322.
(23) Hammar, T.; Hansson, P. A.; Sundberg, C. Climate impact assessment of willow energy from a landscape perspective: a Swedish case study. *GCB Bioenergy* **2017**, *9*, 973−985.
(24) Baker, P.; Charlton, A.; Johnston, C.; Leahy, J. J.; Lindegaard, K.; Pisano, I.; Prendergast, J.; Preskett, D.; Skinner, C. A review of Willow (Salix spp.) as an integrated biorefinery feedstock. *Ind. Crops Prod.* **2022**, *189*, 115823.
(25) Lohtander, T.; Grande, R.; Österberg, M.; Laaksonen, P.; Arola, S. Bioactive Films from Willow Bark Extract and Nanocellulose Double Network Hydrogels. *Front. Chem. Eng.* **2021**, *0*, 30.
(26) Dou, J.; Vuorinen, T.; Koivula, H.; Forsman, N.; Sipponen, M.; Hietala, S. Self-Standing Lignin-Containing Willow Bark Nanocellulose Films for Oxygen Blocking and UV Shielding. *ACS Appl. Nano Mater.* **2021**, *4*, 2921−2929.
(27) Pere, J.; Tammelin, T.; Niemi, P.; Lille, M.; Virtanen, T.; Penttilä, P. A.; Ahvenainen, P.; Grönqvist, S. Production of High Solid Nanocellulose by Enzyme-Aided Fibrillation Coupled with Mild Mechanical Treatment. *ACS Sustain. Chem. Eng.* **2020**, *8*, 18853−18863.
(28) Österberg, M.; Vartiainen, J.; Lucenius, J.; Hippi, U.; Seppälä, J.; Serimaa, R.; Laine, J. A Fast Method to Produce Strong NFC Films as a Platform for Barrier and Functional Materials. *ACS Appl. Mater. Interfaces* **2013**, *5* (11), 4640−4647.
(29) Dou, J.; Xu, W.; Koivisto, J. J.; Mobley, J. K.; Padmakshan, D.; Kögler, M.; Xu, C.; Willför, S.; Ralph, J.; Vuorinen, T. Characteristics of Hot Water Extracts from the Bark of Cultivated Willow (Salix sp.). *ACS Sustain. Chem. Eng.* **2018**, *6*, 5566−5573.
(30) Rittstieg, K.; Suurnakki, A.; Suortti, T.; Kruus, K.; Guebitz, G.; Buchert, J. Investigations on the laccase-catalyzed polymerization of lignin model compounds using size-exclusion HPLC. *Enzyme Microb. Technol.* **2002**, *31* (4), 403−410.
(31) Fliri, L.; Heise, K.; Koso, T.; Todorov, A. R.; del Cerro, D. R.; Hietala, S.; Fiskari, J.; Kilpeläinen, I.; Hummel, M.; King, A. W. T. Solution-state nuclear magnetic resonance spectroscopy of crystalline cellulosic materials using a direct dissolution ionic liquid electrolyte. *Nat. Protoc.* **2023**, *18*, 2084−2123.
(32) Wu, D. H.; Chen, A. D.; Johnson, C. S. An Improved Diffusion-Ordered Spectroscopy Experiment Incorporating Bipolar-Gradient Pulses. *J. Magn. Reason. A* **1995**, *115*, 260−264.
(33) European Standards. Textiles. Solar UV protective properties. Part 1: Method of test for apparel fabrics, 2007.
(34) Gambichler, T.; Laperre, J.; Hoffmann, K. The European standard for sun-protective clothing: EN 13758. *J. Eur. Acad. Dermatol.Venereol.* **2006**, *20*, 125−130.
(35) Re, R.; Pellegrini, N.; Proteggente, A.; Pannala, A.; Yang, M.; Rice-Evans, C. Antioxidant activity applying an improved ABTS radical cation decolorization assay. *Free Radical Biol. Med.* **1999**, *26*, 1231−1237.
(36) Langevin, D. Aqueous foams and foam films stabilised by surfactants. Gravity-free studies. *Comptes. Rendus. Mécanique* **2017**, *345*, 47−55.
(37) Drenckhan, W.; Saint-Jalmes, A. The science of foaming. *Adv. Colloid Interface Sci.* **2015**, *222*, 228−259.
(38) Huynh, N.; Valle-Delgado, J. J.; Fang, W.; Arola, S.; Österberg, M. Tuning the water interactions of cellulose nanofibril hydrogels using willow bark extract. *Carbohydr. Polym.* **2023**, *317*, 121095.
(39) Yang, X.; Jungstedt, E.; Reid, M. S.; Berglund, L. A. Polymer Films from Cellulose Nanofibrils - Effects from Interfibrillar Interphase on Mechanical Behavior. *Macromolecules* **2021**, *54*, 4443−4452.
(40) Rodionova, G.; Eriksen, Ø.; Gregersen, Ø. TEMPO-oxidized cellulose nanofiber films: Effect of surface morphology on water resistance. *Cellulose* **2012**, *19*, 1115−1123.
(41) Karuppusamy, S. A review on trends in production of secondary metabolites from higher plants by in vitro tissue, organ and cell cultures. *J. Med. Plant Res.* **2009**, *3*, 1222−1239.
(42) Li, A. N.; Li, S.; Zhang, Y. J.; Xu, X. R.; Chen, Y. M.; Li, H. bin. Resources and biological activities of natural polyphenols. *Nutrients* **2014**, *6* (12), 6020−6047.
(43) Quideau, S.; Deffieux, D.; Douat-Casassus, C.; Pouységu, L. Plant Polyphenols: Chemical Properties, Biological Activities, and Synthesis. *Angew. Chem., Int. Ed.* **2011**, *50*, 586−621.
(44) Ba, T.; Chaala, A.; Garcia-Perez, M.; Roy, C. Colloidal Properties of Bio-Oils Obtained by Vacuum Pyrolysis of Softwood Bark. Storage Stability. *Energy Fuels* **2004**, *18*, 188−201.
(45) Hoong, Y. B.; Paridah, M. T.; Loh, Y. F.; Jalaluddin, H.; Chuah, L. A. A new source of natural adhesive: Acacia mangium bark extracts co-polymerized with phenol-formaldehyde (PF) for bonding Mempisang (Annonaceae spp.) veneers. *Int. J. Adhes. Adhes.* **2011**, *31*, 164−167.
(46) Dalahmeh, S. S.; Pell, M.; Vinnerås, B.; Hylander, L. D.; Öborn, I.; Jönsson, H. Efficiency of Bark, Activated Charcoal, Foam and Sand

https://doi.org/10.1021/acsomega.3c08906
ACS Omega 2024, 9, 8255−8265

Filters in Reducing Pollutants from Greywater. *Wat. Air Soil Poll.* **2012**, *223*, 3657−3671.
(47) Huang, Y.; Feng, Q.; Ye, C.; Nair, S. S.; Yan, N. Incorporation of ligno-cellulose nanofibrils and bark extractives in water-based coatings for improved wood protection. *Prog. Org. Coat.* **2020**, *138*, 105210.
(48) Dou, J.; Rissanen, M.; Ilina, P.; Mäkkylä, H.; Tammela, P.; Haslinger, S.; Vuorinen, T. Separation of fiber bundles from willow bark using sodium bicarbonate and their novel use in yarns for superior UV protection and antibacterial performance. *Ind. Crops Prod.* **2021**, *164*, 113387.
(49) Albuquerque, B. R.; Heleno, S. A. 8.; Oliveira, M. B. P. P.; Barros, L.; Ferreira, I. C. F. R. Phenolic compounds: current industrial applications, limitations, and future challenges. *Food Funct.* **2021**, *12*, 14−29.
(50) Ciolacu, D.; Ciolacu, F.; Popa, V. I. Amorphous cellulose - Structure and characterization. *Cellul. Chem. Technol.* **2011**, *45* (1−2), 13−21.
(51) Phan, A. D. T.; Netzel, G.; Wang, D.; Flanagan, B. M.; D'Arcy, B. R.; Gidley, M. J. Binding of dietary polyphenols to cellulose: Structural and nutritional aspects. *Food Chem.* **2015**, *171*, 388−396.
(52) Phan, A. D. T.; D'Arcy, B. R.; Gidley, M. J. Polyphenol-cellulose interactions: effects of pH, temperature and salt. *Int. J. Food Sci. Technol.* **2016**, *51*, 203−211.
(53) Yuan, Z.; Wen, Y. Enhancement of hydrophobicity of nanofibrillated cellulose through grafting of alkyl ketene dimer. *Cellulose* **2018**, *25*, 6863−6871.
(54) Seo, W. S.; Cho, N. S. Effect of water content on cellulose/AKD reaction. *Appita J.* **2005**, *58* (2), 122−126.
(55) Koso, T.; Rico del Cerro, D.; Heikkinen, S.; Nypelö, T.; Buffiere, J.; Perea-Buceta, J. E.; Potthast, A.; Rosenau, T.; Heikkinen, H.; Maaheimo, H.; et al. 2D Assignment and quantitative analysis of cellulose and oxidized celluloses using solution-state NMR spectroscopy. *Cellulose* **2020**, *27*, 7929−7953.
(56) Holding, A. J.; Mäkelä, V.; Tolonen, L.; Sixta, H.; Kilpeläinen, I.; King, A. W. T. Solution-State One- and Two-Dimensional NMR Spectroscopy of High-Molecular-Weight Cellulose. *ChemSusChem* **2016**, *9*, 880−892.
(57) Yan, Y.; Amer, H.; Rosenau, T.; Zollfrank, C.; Dörrstein, J.; Jobst, C.; Zimmermann, T.; Keckes, J.; Veigel, S.; Gindl-Altmutter, W.; et al. Dry, hydrophobic microfibrillated cellulose powder obtained in a simple procedure using alkyl ketene dimer. *Cellulose* **2016**, *23*, 1189−1197.
(58) Missio, A. L.; Mattos, B. D.; Ferreira, D. d. F.; Magalhães, W. L.; Bertuol, D. A.; Gatto, D. A.; Petutschnigg, A.; Tondi, G. Nanocellulose-tannin films: From trees to sustainable active packaging. *J. Clean. Prod.* **2018**, *184*, 143−151.
(59) Kwan, I.; Huang, T.; Ek, M.; Seppänen, R.; Skagerlind, P. Bark from Nordic tree species - a sustainable source for amphiphilic polymers and surfactants. *Nord. Pulp Pap. Res. J.* **2022**, *37* (4), 566−575.
(60) Sing, K. S. W.; Everett, D. H.; Haul, R. A. W.; Moscou, L.; Pierotti, R. A.; Rouquerol, J.; et al. Reporting Physisorption Data for Gas/Solid Systems with Special Reference to the Determination of Surface Area and Porosity (Recommendations 1984). *Pure Appl. Chem.* **1985**, *57*, 603−619.
(61) Hill, C. A. S.; Norton, A.; Newman, G. The water vapor sorption behavior of natural fibers. *J. Appl. Polym. Sci.* **2009**, *112*, 1524−1537.
(62) Guo, X.; Wu, Y.; Xie, X. Water vapor sorption properties of cellulose nanocrystals and nanofibers using dynamic vapor sorption apparatus. *Sci. Rep.* **2017**, *7*, 14207.
(63) Mathew, A. P.; Dufresne, A. Plasticized waxy maize starch: Effect of polyols and relative humidity on material properties. *Biomacromolecules* **2002**, *3*, 1101−1108.
(64) Cazón, P.; Velazquez, G.; Vázquez, M. UV-protecting films based on bacterial cellulose, glycerol, and polyvinyl alcohol: effect of water activity on barrier, mechanical and optical properties. *Cellulose* **2020**, *27*, 8199−8213.
(65) Imran, M.; El-Fahmy, S.; Revol-Junelles, A. M.; Desobry, S. Cellulose derivative based active coatings: Effects of nisin and plasticizer on physico-chemical and antimicrobial properties of hydroxypropyl methylcellulose films. *Carbohydr. Polym.* **2010**, *81*, 219−225.

https://doi.org/10.1021/acsomega.3c08906
ACS Omega 2024, 9, 8255−8265